

Numerical Analysis of Flow around Wing Sections PIL15M825 and PIL12M850

Konstantin Metodiev

Space Research and Technology Institute, Bulgarian Academy of Sciences

Abstract. *Current study objective is to compute aerodynamic coefficients of Pilatus PC-9M wing sections. Upon numerical analysis completion, plausible results are expected to emerge such as lift, drag, and pitching moment coefficients as well as a neutral point location along the section chord. The analysis has been carried out by means of a software right to solving problems in computational fluid dynamics. Besides aforementioned quantities, another essential outcome is a polar curve in terms of section form drag, i.e. drag due to both pressure and shear stress. Obtained results at different Reynolds numbers and angles of attack are depicted and discussed thoroughly.*

Key words: Pilatus PC-9M, airfoil, xFoil, drag polar, neutral point

Introduction

Lack of a comprehensive knowledge, widely available to the public, as to what aerodynamic characteristics of above-noted wing sections might be motivated the research completion. The wing sections are said to have been used for designing the wing of Pilatus PC-9M (and that of Beechcraft T-6 Texan II). However, little to no aerodynamic data, limited to a few articles, is available for reference, let alone the wing sections themselves. Huang, [1] somehow assumed in advance that NACA4312 was a good replacement to the original airfoil (PIL15M825) for analysis because both wing sections had very similar aerodynamic characteristics. Snowden et al., [2] developed a flight dynamics model of PC-9/A by means of flight test data. Values of longitudinal derivatives were obtained for complete aircraft configuration. Looking up further in sites containing airfoil coordinates databases, such as UIUC, [3] and Airfoil Tools, [4] yielded no results. Questions regarding wing sections under consideration were posted in public forums by many enthusiasts to no avail.

The wing has following geometrical characteristics: section PIL15M825 at root, PIL12M850 at tip, quarter-chord sweepback 1° , dihedral 7° from center-section, incidence 1° at root, twist -2° , [5]. The wing sections were solely encountered in article [6] and subsequently borrowed for the current research needs with a strong belief that the section geometries are genuine and correct.

Materials and Methods

The project algorithm is further described in succession.

Fluid solver brief description

To carry out computational fluid dynamics research, xFoil, [7] was believed to be appropriate. The bundle contains a solver “for viscous / inviscid analysis and mixed-inverse design of subcritical airfoils ... with a Karman-Tsien compressibility correction,” [8]. A two-dimensional panel method is employed by superposing discrete vortices and sources with constant strength along both wing section and wake. After applying Kutta condition, the algorithm boils down to solving numerically a linear non-homogenous algebraic system. Eventually, the iterative process finishes as soon as a certain convergence criterion is met.

xFoil does not provide a graphical user interface. Instead, a sequence of commands must be fed by the user to the console. The reader is referred to the appendix section to gain a general insight into a simple xFoil session. It is solely important to note that the wing section geometry has been derived by means of a trial version of AutoCAD, [9] and an auxiliary autoLISP script.

Neutral point location

Consider wing section shown in Fig. 1 (respect to Dr. F. H. Lutze, [10]). Aerodynamic forces are equal at either point along the chord including A and B:

$$\begin{aligned} L_A &= L_B = L \\ D_A &= D_B = D \end{aligned} \quad (1)$$

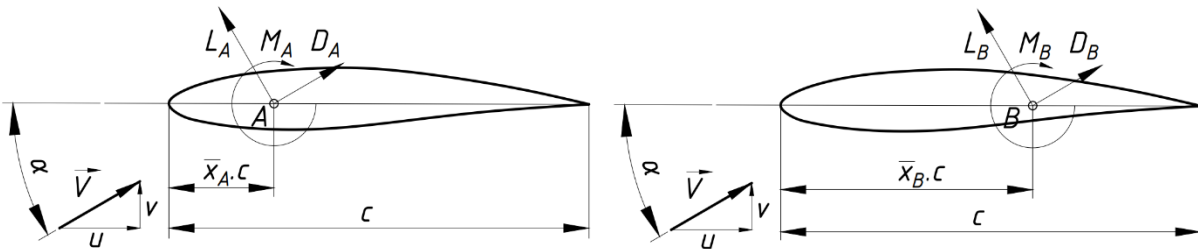


Fig. 1. Aerodynamic forces and moments acting onto an airfoil

It is required to work out value of moment at point A given forces and moment at point B. To this purpose, one may compute equilibrium moment at an arbitrary point along the chord. For instance, moment at the leading edge, due to forces and moments acting at points A and B, is following:

$$\begin{aligned}
M_{LE} &= M_A - L \cdot \bar{x}_A \cdot c \cdot \cos(\alpha) - D \cdot \bar{x}_A \cdot c \cdot \sin(\alpha) \\
M_{LE} &= M_B - L \cdot \bar{x}_B \cdot c \cdot \cos(\alpha) - D \cdot \bar{x}_B \cdot c \cdot \sin(\alpha)
\end{aligned} \tag{2}$$

In eq. (2), both right hand sides are equal, hence the following equality

$$M_A = M_B + L \cdot (\bar{x}_A - \bar{x}_B) \cdot c \cdot \cos(\alpha) + D \cdot (\bar{x}_A - \bar{x}_B) \cdot c \cdot \sin(\alpha) \tag{3}$$

On condition that angle of attack is small, $\sin(\alpha) \approx \alpha$, $\cos(\alpha) \approx 1$, and drag is much less than lift. Consequently, the rightmost term in (3) is second order of accuracy and might be omitted. After dividing by $0.5\rho V^2 Sc$ and assuming simplification mentioned, following dimensionless equation, also known as Rule for Transferring Moments, is obtained:

$$C_{m,A} \approx C_{m,B} + C_l (\bar{x}_A - \bar{x}_B) \tag{4}$$

Rule (4) provides a mean for developer to change location of the reference point and recompute the pitching moment in succession. What is more, the rule is suited for calculating location of a particular point, namely neutral point a.k.a. aerodynamic center. An essential property of the neutral point is that the moment does not vary with regard to altering angle of attack. Having differentiated rule (4), it yields:

$$\frac{dC_{m,AC}}{d\alpha} = \frac{dC_{m,B}}{d\alpha} + \frac{dC_l}{d\alpha} (\bar{x}_{AC} - \bar{x}_B) = 0 \tag{5}$$

Therefore, the neutral point is located at (dimensionless fraction of section chord)

$$\bar{x}_{AC} = \bar{x}_B - \frac{dC_{m,B}}{dC_l} \tag{6}$$

Reynolds number influence over drag polar

Reynolds number is an important factor affecting drag polar outline. Broadly speaking, as the Reynolds number becomes bigger, so does the lift coefficient, and so the drag coefficient declines slightly. This phenomenon might be accounted for by boundary layer transition, [11]. The laminar boundary layer is notable for low kinetic energy and prone strongly to separation and vortex formation. In this case, a smooth flow around the airfoil is less likely to be observed. The drag is high and the lift is low. Whenever Reynolds number exceeds a critical value, the transition zone moves to a new location well ahead of the separation point. The flow sticks onto the airfoil surface and lift increases.

Validation

xFoil is held in high esteem and regard for achieved computational accuracy and precision. In current research, testing the solver against exact flow cases is thought to be rather redundant with good reason. xFoil is supposed to have been validated prior to release. In addition, some test results were already compared with wind tunnel data at different Reynolds numbers by means of four noteworthy wing sections. The results might be found in page [12].

Given basic assumptions, the used numerical solver is accurate and precise enough. Hence, the exposé goes on to find numerical solution of the main problem.

Results

In xFoil, reference area of 1 m^2 is assumed in advance while Reynolds number and chord length are to be explicitly filled in. The chord length might be set to 1 by toggling NORM command. The center of rotation is placed at section leading edge (XYCM dialog).

In following Table 1, values of aerodynamic coefficients, obtained after numerical analysis completion, might be found with regard to both wing sections.

Table 1. Aerodynamic coefficients at various angles of attack

	PIL15M825, Re = 0.250E+06			PIL12M850, Re = 0.250E+06		
alpha, deg	CL	CD	CM	CL	CD	CM
-5	-0.3433	0.01244	0.023	-0.2269	0.01373	-0.0358
-4	-0.2102	0.01185	-0.0139	-0.1024	0.01179	-0.0701
-3	-0.0853	0.01133	-0.0469	0.0112	0.01193	-0.0975
-2	0.0291	0.01105	-0.0755	0.1186	0.012	-0.1224
-1	0.1389	0.01097	-0.1022	0.2258	0.0121	-0.1473
0	0.2489	0.01091	-0.1291	0.3342	0.01223	-0.1731
1	0.3551	0.01098	-0.1544	0.4428	0.01229	-0.199
2	0.4635	0.01101	-0.1805	0.5528	0.01229	-0.2259
3	0.566	0.01092	-0.2038	0.6624	0.01228	-0.2524
4	0.6649	0.01071	-0.2249	0.7712	0.01267	-0.2787
5	0.8352	0.0109	-0.2792	0.8772	0.01305	-0.3037
6	0.888	0.01175	-0.2803	0.9757	0.01292	-0.3249
7	0.9186	0.01432	-0.2727	1.0596	0.01324	-0.3398
8	0.9574	0.01657	-0.2694	1.0919	0.01873	-0.3365
9	0.9914	0.01998	-0.266	1.1161	0.02365	-0.3296
10	1.0173	0.02473	-0.2611	1.1435	0.02905	-0.3263

In Fig. 2, drag polar is depicted (blue), so is the pitch moment coefficient (orange), for wing section PIL15M825. The angle of attack varies within -5° to 10° . In Fig. 3, similar graph is shown for PIL12M850. Maximum lift-to-drag ratio 76 ... 80 is achieved at angle of attack 5° ... 7° . Exact values are shown in the graphs.

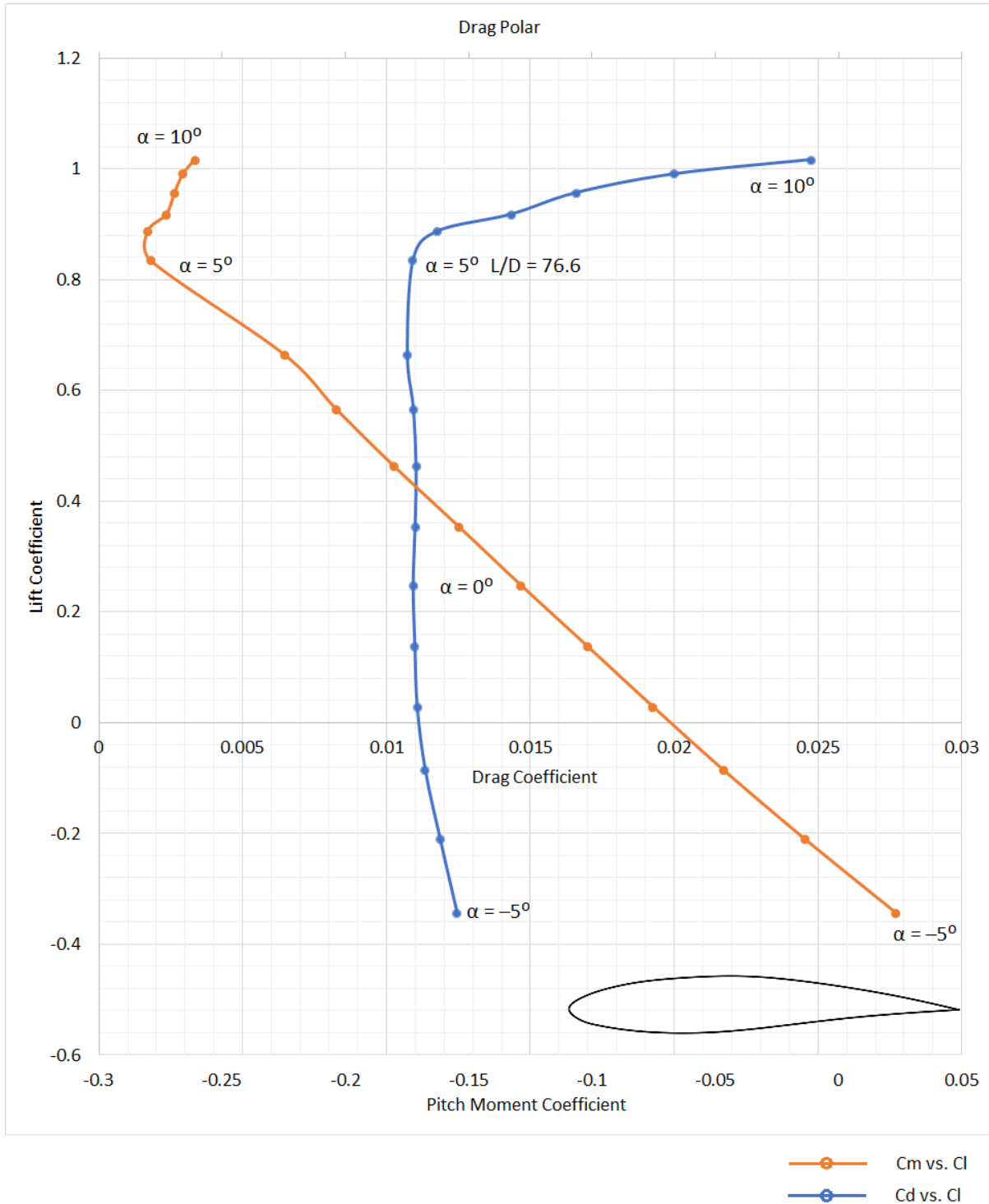


Fig. 2. Drag polar, PIL15M825, $Re = 0.250E+06$

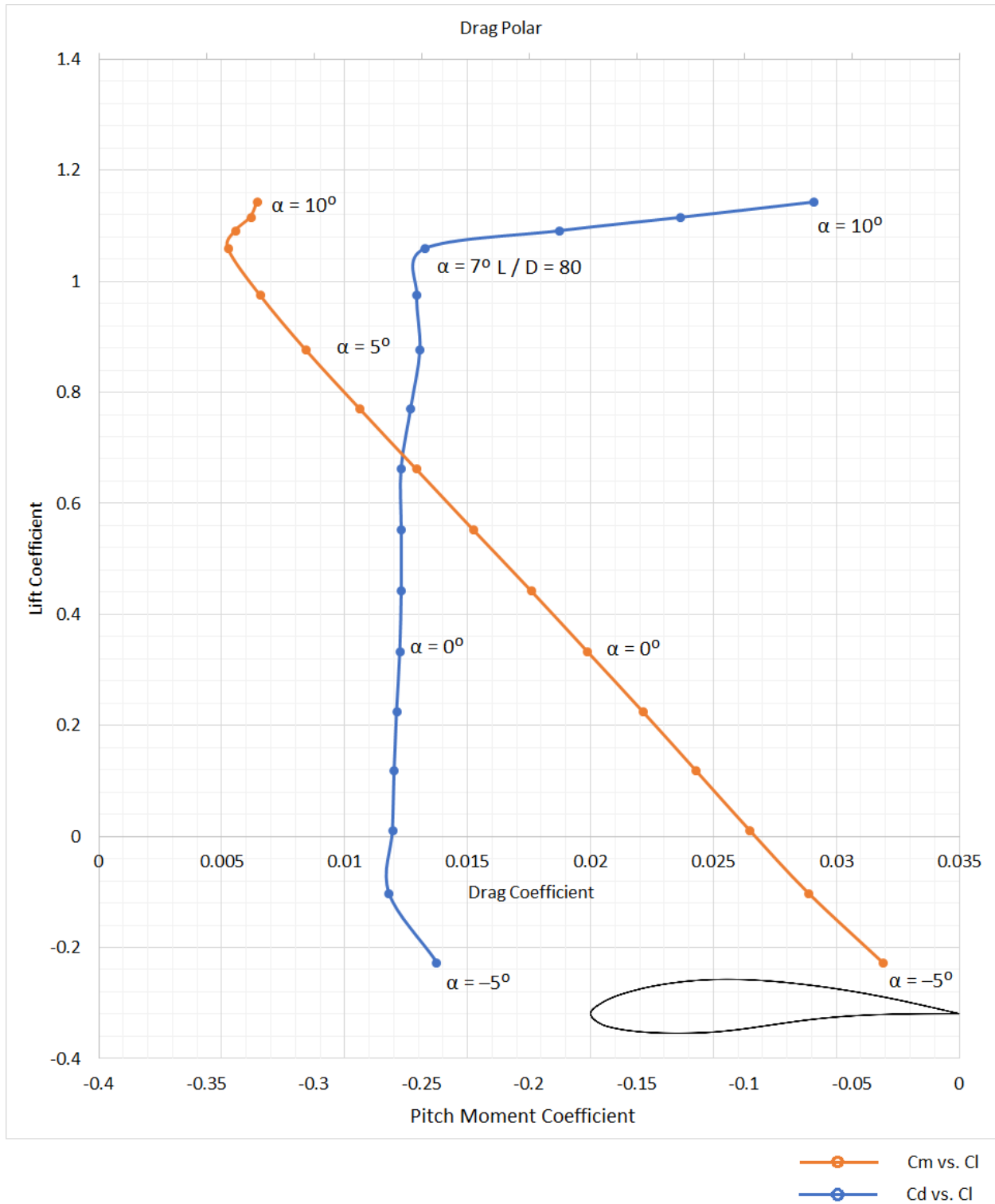


Fig. 3. Drag polar, PIL12M850, $Re = 0.250E+06$

In Fig. 4, drag polar graphs are depicted at different Reynolds numbers for PIL15M825 wing section.

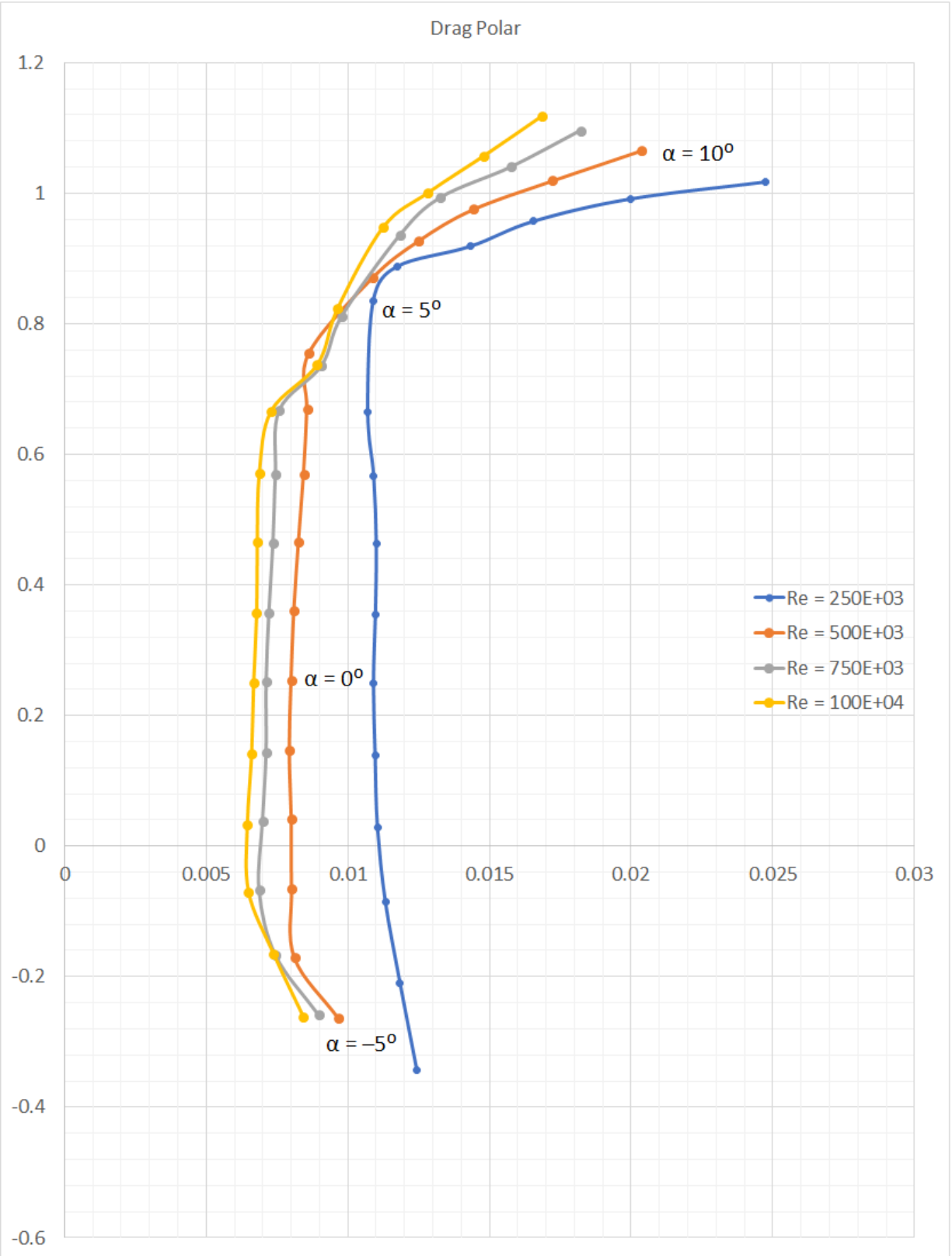


Fig. 4. Drag polar curves with reference to Reynolds number, PIL15M825

In following Table 2, location of neutral point is reported. Both values were computed according to eq. (6). The reference center of rotation is $\bar{x}_B = 0$. It was possible to work out value of derivative dC_m/dC_l for the simple reason that pitching moment coefficient changes linearly within wide range of values of angle of attack.

Table 2. Neutral point location

	PIL15M825	PIL12M850
\bar{x}_{AC} (times chord)	0.247	0.232

In following Fig. 5, static pressure coefficient contours are shown, $Re = 250E+03$. The angle of attack varies within $-5^\circ \dots 10^\circ$ interval, hence multiple graphs. Abruptly changing curvature of the wing section contour (i.e. osculating circle radii raised to a power of -1) explains small ripples arising along each graph. In Fig. 5, positions of free transitions (top Xtr, bot Xtr) from laminar to turbulent boundary layer are displayed, so is transition criterion N_{cr} .

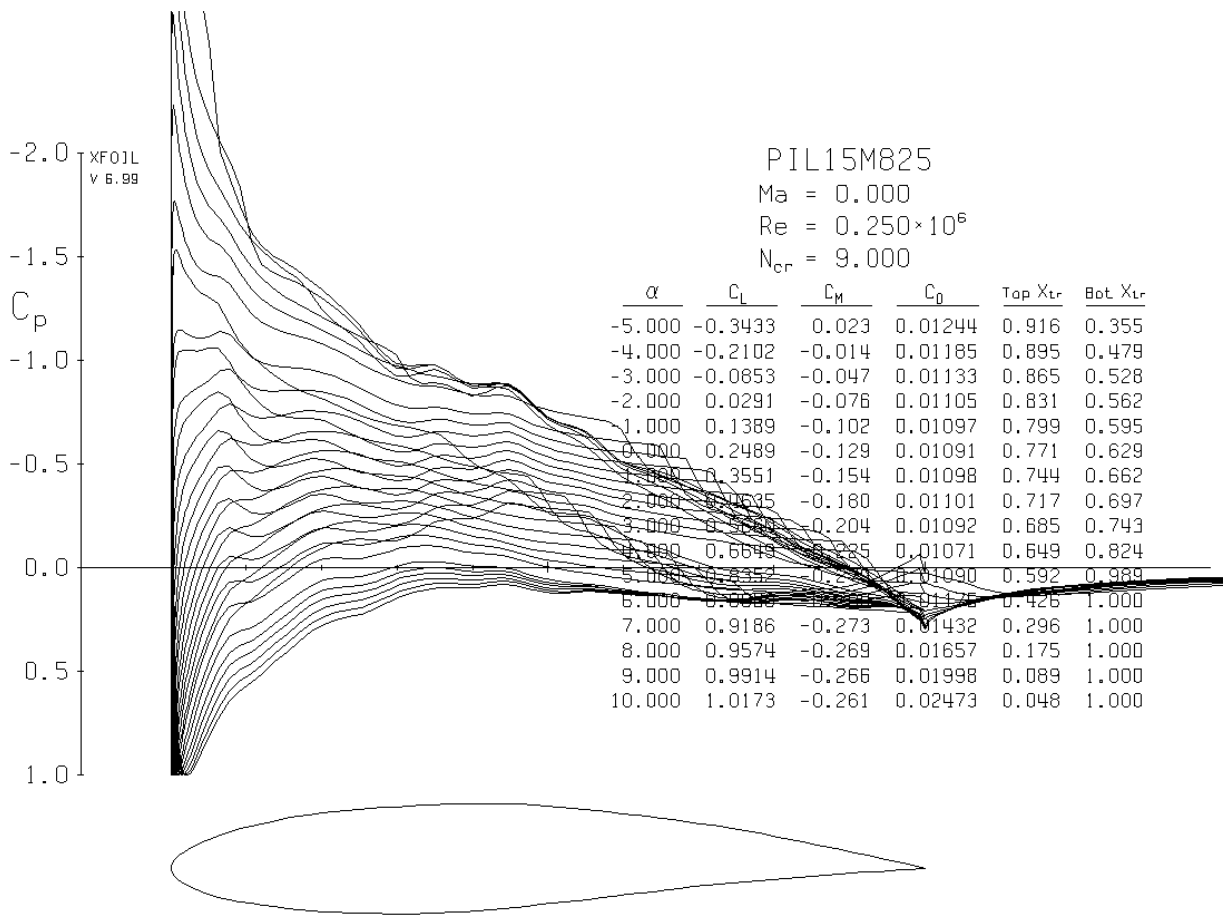


Fig. 5. Pressure coefficient contours at various angles of attack, PIL15M825

Discourse

To decide to accept the leading edge (from among other points) as a reference point of rotation proved to be the best choice. According to experience, derivative dC_m/dC_l is liable to change its sign intensively as long as the reference point closes in on the neutral point location approximately at 0.25 times chord.

Prediction of boundary layer transition is another remarkable ability of xFoil. Two transition modes are supported: forced and free. In current case study, latter mode was adopted for obvious reason. Therefore, it is somewhat desirable for the project to keep on growing by experimenting with forced transition locations in terms of real surface roughness.

The research aimed to fill in the gaps currently existing in publicly available knowledge about Pilatus PC-9M aircraft.

References

- [1] Huang, A., Aircraft Load Models for a Pilatus PC-9 Based on Wind Tunnel Testing, A98-31707, para. 2.1, ICAS-98-7,6,1, AIAA, 1998
http://www.icas.org/ICAS_ARCHIVE/ICAS1998/PAPERS/761.PDF
- [2] Snowden, A., H. Keating, N. van Bronswijk, J. Drobik, A Correlation between Flight Determined Longitudinal Derivatives and Ground-based Data for the Pilatus PC 9/A Training Aircraft in Cruise Configuration, DSTO-TR-0937, AR № AR-011-205, 2000
<https://apps.dtic.mil/sti/pdfs/ADA376020.pdf>
- [3] https://m-selig.ae.illinois.edu/ads/coord_database.html
- [4] <http://airfoiltools.com/>
- [5] <https://janes.migavia.com/che/pilatus/pc-9m.html>
- [6] White paper, PC-9M, The Advanced Trainer Model Building Plan 1:25, Pilatus Aircraft Ltd.
- [7] <https://web.mit.edu/drela/Public/web/xfoil/>
- [8] Drela, M., xFoil: An Analysis and Design System for Low Reynolds Number Airfoils, Low Reynolds Number Aerodynamics, Springer – Verlag, Lec. Notes in Eng. 54, 1989
- [9] <https://www.autodesk.com/products/autocad/free-trial>
- [10] <http://www.dept.aoe.vt.edu/~lutze/AOE3104/airfoilwings.pdf>
- [11] Popov, M., Hydrodynamics, 2nd edition, “Technics” Publishing House, 1962, p. 323, in Bulgarian
- [12] <https://aerofoilengineering.com/Validation.php>

Nomenclature

V – free stream velocity
u, v – Cartesian components of V
 ρ – fluid density
alpha – angle of attack
c – section cord
S – planform area
x – longitudinal coordinate
L – lift
D – drag
M – pitching moment
Cl – lift coefficient
Cd – drag coefficient
Cm – pitching moment coefficient

Superscripts:

– dimensionless value

Appendix. An exemplary xFoil session (abridged)

```
XFOIL c> load pil15m825.prn
...
XFOIL c> ppar
...
Change what? (<cr> if nothing else) c> N 160
...
XFOIL c> norm
Loaded airfoil will be normalized
XFOIL c> xycm
Enter new CM reference X r> 0
Enter new CM reference Y r> 0
XFOIL c> oper
OPERi c> iter
Current iteration limit: 10
Enter new iteration limit i> 400
OPERi c> visc
Enter Reynolds number r> 250000
...
OPERv c> aseq -5 10 1
```